Original Article
The protection of acetylcholinesterase inhibitor on β-amyloid-induced injury of neurite outgrowth via regulating axon guidance related genes expression in neuronal cells

Jiao-Ning Shen[1], Deng-Shun Wang, Rui Wang[1]

[1]Department of Pharmaceutical Sciences, School of Pharmacy, Shanghai Key Laboratory of New Drug Design, East China University of Science and Technology, Shanghai 200237, China; [2]Department of Pathology and Laboratory Medicine, School of Medicine and Public Health, University of Wisconsin, Madison, Wisconsin, USA

Abstract: Cognitive deficits in AD correlate with progressive synaptic dysfunction and loss. The Rho family of small GTPases, including Rho, Rac, and Cdc42, has a central role in cellular motility and cytokinesis. Acetylcholinesterase inhibitor has been found to protect cells against a broad range of reagents-induced injuries. Present studies examined if the effect of HupA on neurite outgrowth in Aβ-treated neuronal cells executed via regulating Rho-GTPase mediated axon guidance relative gene expression. Affymetrix cDNA microarray assay followed by real-time RT-PCR and Western Blotting analysis were used to elucidate and analyze the signaling pathway involved in Aβ and HupA's effects. The effects of Aβ and HupA on the neurite outgrowth were further confirmed via immunofluorescence staining. Aβ up-regulated the mRNA expressions of NFAT5, LIMK1, EPHA1, NTN4 and RAC2 markedly in SH-SY5Y cells. Co-incubation of Aβ and HupA reversed or decreased the changes of NFAT5, NTN4, RAC2, CDC42 and SEMA4F. HupA treated alone increased NFAT5, LIMK1, NTN4 significantly. Following qRT-PCR validation showed that the correlation of the gene expression ratio between microarray and qRT-PCR is significant. Western blot result showed that the change of CDC42 protein is consistent with the mRNA level while RAC2 is not. The morphological results confirmed that HupA improved, or partly reversed, the Aβ-induced damage of neurite outgrowth. The protective effect of HupA from Aβ induced morphological injury might be correlative to, at least partially, regulating the network of neurite outgrowth related genes.

Keywords: β-amyloid, axon guidance, neurite outgrowth, acetylcholinesterase inhibitor, huperzine A

Introduction

Alzheimer's disease (AD) is the leading cause of dementia among the elderly and is characterized by accumulation of extracellular and vascular amyloid in the brain [1]. The key symptoms of AD are primarily caused by cholinergic dysfunction. A significant correlation has been found between a decrease in cortical cholinergic activity and the deterioration of mental test scores in patients with AD [1]. Cognitive deficits in AD correlate with progressive synaptic dysfunction and loss that may be initiated by soluble β-amyloid peptide and driven further by the accumulating neuropathological hallmarks, including intraneuronal neurofibrillary tangles,

extracellular amyloid plaques, and neuron loss [1-3]. Both dystrophic neurites and dendritic spine loss are observed in AD and many mental retardation syndromes [3-8]. Soluble Aβ or Aβ oligomers correlates highly with synapse loss and the degree of dementia [9-17]. The evidence indicated that deregulation of Rho GTPase pathway is implicated in several pathological conditions, including neurodegenerative disorders like AD [4, 18]. The translocation of the GTPase to neurofibrillary tangles in dystrophic neuritis correlates with neuronal dystrophy reported in Alzheimer's disease and AβPP overexpressing mice [19]. There is evidence that Rho GTPase activity regulates the formation of Aβ peptides during disease progression

[20]. This pathology is characterized by a progressive loss in the number of dendritic spines, as well as by alterations in the synaptic efficacy and damage at the synaptic terminal [4, 10]. Dendritic spines, major sites of synaptic contacts, are structurally reliant on the actin cytoskeleton. The dynamic regulation of actin polymerization is considered the main mechanism underlying morphological changes in dendritic spines. The Rho family of small GTPases, including Rho, Rac, and Cdc42, has a central role in cellular motility and cytokinesis due to its involvement in the regulation of actin cytoskeletal dynamics [21-25]. Rac/Cdc42 inhibits axon growth via the effector kinases p21-activated kinases (PAK) Rho or Rho-associated protein kinase (Rock) [18, 26, 27]. Previous studies demonstrated Aβ oligomers can also interfere with Rac and Cdc42 signaling and induce the loss of actin polymerization and of dendritic spines [20]. The evidence indicated that the β-site amyloid precursor protein cleaving enzyme 1 (BACE1) which is necessary to generate the Aβ peptide is play a central role in axon guidance [28, 29].

Huperzine A (HupA), isolated from Chinese herb Huperzia serrata, is a potent, highly specific and reversible inhibitor of acetylcholinesterase [30]. It has been found to reverse or attenuate cognitive deficits in a broad range of animal models [31-33] and patients including aged subjects, patients with benign senescent forgetfulness, Alzheimer's disease (AD) and vascular dementia (VD), with minimal peripheral cholinergic side effects compared with other AChEIs in use [30]. Besides the above mentioned AChE inhibiting effect, HupA possesses the ability, from our recent studies, to protect cells against hydrogen peroxide, β-amyloid protein (or peptide), glutamate, ischemia and staurosporine-induced cytotoxicity and apoptosis [31-35]. These protective effects are related to its ability to attenuate oxidative stress, regulate the expression of apoptotic proteins Bcl-2, Bax, P53 and caspase-3, protect mitochondria, and interfere with APP metabolism [30]. In addition to its AChE inhibition and antioxidation, the neuroprotective effect of HupA also involves other mechanisms, including targeting of the Wnt/β-catenin signaling pathway in AD brain [36]. It has been suggested that that AChE inhibitors are known to exert NGF-like activities by potentiating the neuritogenic effect of NGF

[37]. Our previous studies also showed that HupA increased neurite outgrowth from undifferentiated PC12 cells [38]. As p75[NTR] interactors, it is well known that Rho GTPase family is involved in NGF signaling [39]. Recently, the study has shown that HupA treatment reduces synaptic deficits and Aβ-related pathological alterations, including Aβ deposition and oligomerization. This encourages us to explore the further mechanism. We presume that the effect of HupA on neurite outgrowth in Aβ-treated neuroblastoma might be executed via regulating Rho-GTPase mediated axon guidance relative gene expression. In order to elucidate and analyze the signaling pathway involved in HupA's effects, an Affymetrix cDNA microarray assay followed by real-time RT-PCR, Western Blotting and immunofluorescence staining analysis were carried out. Expectedly, HupA reversed Aβ-induced changes in axon guidance relative gene expression, which might play an important role in its neuroprotective mechanism.

Material and methods

Cell culture and treatments

SH-SY5Y neuroblastoma cells, obtained from the American Type Culture Collection (ATCC), were maintained in a humidified atmosphere of 95% air and 5% CO_2 at 37°C. Cells were seeded into 100 mm dishes (2×10^4 cells per ml) in DMEM/F12 (1:1) medium, supplemented with 10% (v/v) fetal bovine serum (FBS), 100 U/ml penicillin, and 100 μg/ml streptomycin. Experiments were carried out 24–48 h after cells were seeded.

It has been well established that the truncated amyloidogenic peptide Aβ25-35 plays a key role in the pathogenesis of AD. Recently, Kaminsky et al [40] and Gulyaeva NV et al [41] presented analytical reviews on the proposed involvement of Aβ25–35 as a key player in pathogenesis of Alzheimer's disease (AD). The authors provide a large body of evidence for the hypothesis that Aβ25–35 is a proxyholder for amyloidogenic peptides, using primarily the data of in vitro and in vivo experiments. Aβ25–35 peptide is effective on behavior, neuronal plasticity and cell death, as well as cholinergic system, and oxidative stress. Our previous reports are consistent with the hypothesis [30, 34, 35]. Based on the up-mentioned reports,

Table 1. Primer sequences used for real-time RT-PCR

Gene bank ID	Gene title	Primer forward	Primer reverse
NM_001619	ADRBK1	CGATGAGGAGGACACAAAAGG	TCTGTCTCAGCGTTGATGGTG
NM_006464	TGOLN2	ACCTGATGCCAGATGCTATGG	GCAAGTCACGCCAAATCCAA
NM_002588	PCDHGC3	AGTGTTGGTGGAGGTTGTGGA	CACACTGAGCAAAGCGATGAC
NM_003255	TIMP2	TCATTCGTCTCCCGTCTTTG	GCACGGTTAAAAGACCAACGT
NM_001164	A4	GAAACGATGCTCTCATGCCAT	TCGTTTTCTGTGTTGGCTGG
NM_006732	FOSB	AGCGAGCCGTTGAATTGGA	ACAGGCGGAGGAGAAAAGACA
NM_003790	TNFRSF25	TTGCAGAAGCCCTAAGTACGG	TTCGTGCTTCTTCGCCTTG
NM_003053	SLC18A1	GCATAGTCCCAACAGATCGGA	CTGGCATTTGGCAGCAAGA
NM_003381	VIP	TGCTGATGGAGTTTTCACCAG	GACTGCATCTGAGTGACGTTTG
NM_020686	ABAT	GCATCAGGAAATCGGATGGAG	TGCTTGGTGAACTCTGGCTCAT
NM_001909	CTSD	CCCGACTTGCTGTTTTGTTCT	CCAATGCACGAAACAGATCTG
NM_005007	NFKBIL1	TTCCGAAGCCAGATTGAGACC	CCCCGAAGTTTCTTGCTTCTT
NM_001348	DAPK3	CGAGGAGTACTTCAGCAACACC	CGCCTTAATCCAGGAATGTTC
NM_001167942.1	TNFAIP8L1	GTTGGCTGGTTGGTTGCTGAT	AAAAGCTGCTGCCTCCCACTT
NM_005954	MT3	GTGTGGAGCACGTGGAGATAGT	TCATTCCTCCAAGGTCAGCAG
NM_005921.1	MAP3K1	TGCTAATTGACAGCACTGGTCA	TACCTCAGGTGCCATAAATGCA
NM_014841	SNAP91	GTTGTCATACTGTCTGTGCTGATGG	CAAACACCTTTCCAACCCAATATG
NM_003179	SYP	GCCTGAGAAGAGTCGAGTGATATGG	CCGTTGGTTCTGTCCTCCTATTAAC
NM_021229	NTN4	ACTCCAGTCCTTTTCCATGCA	GCGAAGGTTGGTGATCTTCAG
NM_044472.2	CDC42	CTCCGGAAACTCAACCCAAA	GACGCAGAGGCTTTCAAACAG
NM_004263	SEMA4F	CAGTGCTGAATGGTCCCTTCA	TGCCGGAGCTTCATGTTGTT
NM_002314	LIMK1	TGGTCCGCGAGAACAAGAAT	TTGCGGTCTGGCTTCTTGA
NM_002577	PAK2	AGGCTGTGCTGGATGTCCTAA	TGGCATTCAGTGCTGGTGTT
NM_002872	RAC2	CCTGTGGCGTTTCTTAGCAGA	GGATGCAGCACCTGCAAAT
NM_005232	EPHA1	ATCTTCACCACAGCCAGCGAT	CAACCGGTACCCATCCTCAAT
NM_006599	NFAT5	CACAGCGGTGGTGCTTAAAGA	TTTGCAGTCCTCAGTGCCACT
Z29373	L1NCAM*	CCCTTTCGCCACAGTATGTCA	GCCGGAACATCCTCTCCTT AA
NM_014364	GAPDH	TGACTTCAACAGCGACACCCA	CACCCTGTTGCTGTAGCCAAA
NM_001101.2	ACTB	TTGTTACAGGAAGTCCCTTGCC	ATGCTATCACCTCCCCTGTGTG

*The neural cell adhesion molecule L1.

amyloid β- peptide fragment 25-35 was used in the following experiments.

Active amyloid β peptide fragment 25-35 (Aβ25-35) was purchased from Sigma, dissolved in dH_2O and aged by incubating in 37°C for 72 hours. Working solutions were diluted in phosphate-buffered saline (PBS) before using. Huperzine A (HupA), a colorless powder with m.p. 230 °C, and purity >99%, was dissolved and diluted in PBS. Pre-incubation with HupA was conducted 2 h before Aβ (10 μM) addition. HupA treated alone and PBS treated cells were used as controls. The cells were harvested for the further assays and detections after 24 h exposure of Aβ.

RNA extraction and cDNA microarray

Total RNA from the cells treated with PBS, HupA alone and Aβ with/without HupA co-treated was isolated using the RNeasy Mini Kit (Qiagen Inc., Valencia, CA) according to the manufacturer's instructions with DNase I digestion to remove genomic DNA. cRNA is prepared according to Affymetrix protocols. Briefly, total RNA (10 μg) is first reverse transcribed using a T7-Oligo(dT) Promoter Primer in the first-strand cDNA synthesis reaction with One-Cycle cDNA Synthesis Kit (QIAGEN, Valencia, CA). Following RNase H-mediated second-strand cDNA synthesis (Two-Cycle cDNA Synthesis Kit), the double-stranded cDNA is purified and serves as a template in the sub-

sequent in vitro transcription (IVT) reaction (MEGAscript® T7 Kit, Ambion, Inc., Austin, TX). The IVT reaction is carried out in the presence of T7 RNA Polymerase and a biotinylated nucleotide analog/ribonucleotide mix for complementary RNA (cRNA) amplification and biotin labeling. The biotinylated cRNA targets were then cleaned up (IVT cRNA Cleanup Kit), fragmented, and hybridized to GeneChip expression arrays.

Gene expression was measured by hybridization to Human Genome U133A (HG-U133A) Gene Chip DNA microarrays (Affymetrix, Santa Clara, CA, USA), containing 33,000 human genes to identify those that are uniquely expressed in the cells with different treatments. Differences in gene expression among groups were calculated with Affymetrix GeneChip® Operating Software (GCOS).

Real time RT-PCR

RNA was extracted using the TRIzol reagent. The concentration of nucleic acids was determined spectrophotometrically at 260 nm and 280 nm, taking into account the dilution factor. RQ1 RNase-free DNase (Promega) was used to remove relict of DNA which might interfere the output of PCR. For the PCR first strand synthesis was performed using the Omiscript® RT Kit (Qiagen Inc.). Real time PCR was performed in 0.2 ml thin wall PCR plates using the ABI PRISM 7000 Sequence Detection System and carried out with SYBR® Green PCR Core Reagents (TAKARA) according to the manufacturer's instructions. The standard reaction mix consisted of SYBR Green supermix, forward and reverse primers at a final concentration of 5 pM each, 1 ng DNA template, DNase free water to give final volume of 20 μl. The mixture was kept in 50°C for 2 min and heated to 95°C for 10 min followed by 35 cycles with denaturation at 95°C for 15 s, annealing at 60°C for 1 min and extension at 72°C for 30 s. A group of genes were randomly selected to confirm the array results. Primer sequences used for real-time RT-PCR are listed in **Table 1**. Human GAPDH was used as reference gene. Relative quantification of genes expression was carried out by comparative Ct method according to manufacturer's protocol. Briefly, the genes mRNA level was expressed in cycle threshold (Ct) value; the Ct values for each sample were averaged from duplicate. Differences between the mean Ct

values of target genes and reference gene were calculated as $\Delta Ct_{sample} = Ct_{target} - Ct_{gapdh}$ for different treated groups, and that of the ΔCt for the control groups were set for calibrator ($\Delta Ct_{calibrator}$). Final results, the sample-calibrator ratio, expressed as N-fold differences of target genes expression in Aβ group compared with control, were determined as $2^{-(\Delta Ct\ sample\ -\ \Delta Ct\ calibrator)}$.

Western blotting

After incubation with PBS, Aβ, HupA alone or with Aβ for 24 h, cells were harvested, lysed in Passive Lysis Buffer containing protease inhibitors cocktail (Sigma P8430). Lysates were incubated for 30 min on ice, and then centrifuged at 10,000 X g for 10 min at 4°C. Protein concentration in the supernatant was determined by Coomassie blue protein binding method using protein quantification Kit-rapid (Sigma/Fluka) with bovine serum albumin as standard. The same amount of protein from different groups was used for immunoblotting. Samples were denatured in protein sample buffer (100 mM Tris-Cl pH 6.8, 4% SDS, 0.2% bromophenol blue, 20% glycerol, 20% H2O, 200 mM DTT) at 100°C for 10 min and loaded, separated on 10% SDS–polyacrylamide gels and transferred to nitrocellulose membranes in a Bio-Rad electrophoresis system. After blocking with TBST (Tris-buffered saline with 0.1% Tween) containing 5% non-fat milk, the membranes were kept at 4°C overnight with primary antibodies (1:5000 for β-ACTIN, 1:2000 for RAC1 and 1:1000 for RAC2 and CDC42, respectively), followed by HRP-conjugated second antibodies (1:5000 to 1:10000 dilution) at room temperature for 2 h. The target protein bands were detected using the ECL Western blotting detection system (Pierce) and autoradiography film (Fisher). The density of the RAC1, RAC2, CDC42 and β-ACTIN blotting bands were quantified by ImageJ software (1.37v, Wayne Rasband, National Institutes of Health, USA) as described [42].

Induction of neurite outgrowth

Undifferentiated PC12 rat pheochromocytoma cells were obtained from ATCC. The cells were maintained in DMEM media containing 10% (v/v) fetal bovine serum (FBS) (Gibco), 5% (v/v) horse serum (HS) (Gibco), 2mM glutamine (Gibco), 100 U/mL penicillin, and 100 μg/mL

Table 2. Aβ alters the axon guidance relative gene expression profile in SH-SY5Y cells

GenBank ID	Symbol	Gene title	Fold changes		
			Aβ	Aβ+HupA	HupA
NM_006599	NFAT5	Nuclear factor of activated T-cells 5, tonicity-responsive	1.84	1.15	2.03
NM_002314	LIMK1	LIM domain kinase 1	1.85	1.89	1.82
NM_005232	EPHA1	EPH receptor A1	2.00	2.08	1.28
NM_021229	NTN4	Netrin 4	3.85	2.14	2.00
NM_002872	RAC2	small GTP binding protein Rac2	2.02	0.47	0.787
NM_044472.2	CDC42	Cell division cycle 42	0.57	1.61	0.97
NM_004263	SEMA4F	Sema domain, immunoglobulin domain (Ig), transmembrane domain (TM) and short cytoplasmic domain	0.87	2.16	0.76
NM_002577	PAK2	p21 (CDKN1A)-activated kinase 2	0.82	0.85	0.52
Z29373	L1CAM*	neural cell adhesion molecule L1	0.94	1.15	0.56

*The neural cell adhesion molecule L1.

streptomycin (Gibco) in a humidified atmosphere of 95% air and 5% CO_2 at 37°C. Cells (1×10^4 cells/well) were seeded in glass cover slips into a 12-well plate and cultured overnight. Subsequently the cells were washed twice with phosphate-buffered saline solution (PBS) and transferred to fresh serum-starved DMEM containing 1% HS, 0.5% FBS. After 2 h incubation with serum-starved DMEM, 100 ng/ml NGF(SinoBio, shanghai) was added to the cultures, which were incubated for 48 h. Cells were washed twice with PBS to remove NGF and replaced with 1μM Aβ1-42 (QiangYao, Shanghai) with or without Hup A for a further 48h. Pre-incubation with HupA (1 and 10 μ M) was conducted 2 hours before Aβ addition. Exposure to vehicle alone (culture medium) was used as the control. The cells were harvested for the further assays and detections after 48 h exposure of Aβ.

Immunofluorescence staining

PC12 cells cultured in glass cover slips were treated in serum-starved media for 2 days at 37°C under 95% air and 5% CO_2. The cells were then washed with PBS and fixed with ice cold acetone for 30 min at -20°C. The cells were blocked with blocking buffer containing 5% BSA and 0.1% Triton X-100 for 30 min at RT. For double immunofluorescence staining, the cells were incubated with primary rabbit anti-MAP2 antibody (Abcam, 1:200) overnight at 4°C. Alexa Fluor 546 goat anti-rabbit IgG (H + L) (Invitrogen, 1:4000) was incubated at RT for 1 h. After rinsing with PBS and blocked with 5% BSA/PBS, cells were incubated with Alexa Fluor

488 conjugated anti-Tau-1 antibody (Millipore, 1:100) for 2h at RT. The nuclei were counter-stained with VECTASHIELD® Mounting Medium with DAPI (1.5 μg/mL, Vector Laboratories, Inc.), and then the cells were photographed and analyzed with a fluorescent microscope (Nikon, ELWD 0.3, Japan). At least 3 independent immunofluorescence staining was performed to assess the reproducibility of the results.

Measurement of neurite outgrowth

Cell processes were defined as neurites when longer than the diameter of the cell body. The percentage of neurite-bearing cells in relation to the total number of cells was examined in 6-8 fields with an average of 15 cells per field under per treatment condition. After double immunofluorescence staining, neurites (dendrite and axon) formation was photographed and analyzed with a fluorescent microscope, and processes longer than one cell diameter were scored as neurites. Neurite length was determined by manually tracing the length of the longest neurite per cell using the ImageJ software (version 1.45s, NIH, USA) for neurite-bearing cells. At least 50 cells were randomly measured for each group.

Statistical analysis

All results are presented as mean ± SEM. Statistical analyses were performed with one-way ANOVA followed by least significant difference post hoc analysis or Duncan's multiple-range test and t-test with threshold of $p < 0.05$. The results from individual experiments were averaged within each experimental group.
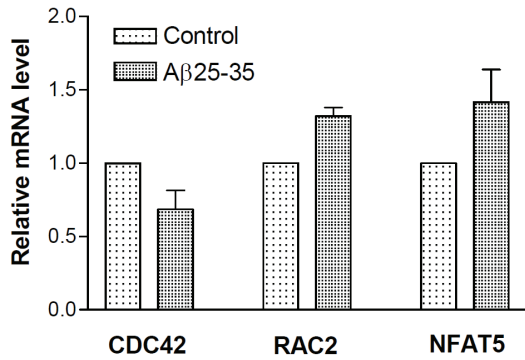
Figure 1. Aβ down-regulated CDC42 and up-regulated RAC2 and NFAT5 mRNA levels. SH-SY5Y cells were treated with PBS, Aβ, HupA alone or with Aβ for 24 h, respectively. Total RNA was extracted and analyzed by real-time RT-PCR and normalized to Human GAPDH mRNA levels. Shown are mean ± SEM of relative mRNA level.

Results

Changes of axon guidance relative genes expression after the treatment of Aβ peptide with/without HupA

Using cDNA microarray, the gene expression profile was detected in Aβ with/without HupA and HupA alone treated human SH-SY5Y cells. Array data were verified by measuring the expression using quantitative RT–PCR. We randomly selected a group of genes to confirm the microarray data. PCR result showed that relative expression ratios of these genes determined by real-time quantitative RT–PCR were concordant with the expression levels observed in the corresponding microarray data. The correlation of the gene expression ratio between microarray ratio and qRT-PCR ratio is significant (P<0.0001). Interestingly, among more than 100 up or down regulated genes after the treatments above (data not shown), the genes involved in axon guidance were significantly regulated. RAC/Cdc42-PAK and RAC/Cdc42-ROCK pathway were affected which involved in axon attraction, axon repulsion and axon outgrowth (figure not shown). Aβ up-regulated the mRNA expressions of NFAT5, LIMK1, EPHA1, NTN4 and Rac2 markedly, but decreased Cdc42 expression. Co-incubation of Aβ and HupA reversed or decreased the changes of NFAT5, NTN4, RAC2, CDC42 and SEMA4F. HupA treated alone increased NFAT5, LIMK1, NTN4 significantly, but decreased RAC2, SEMA4F, PAK2 and LICAM (**Table 2**).

Among the verified genes, axon guidance relative genes Cdc42, Rac2 and NFAT5 mRNA levels are coincidence with the array data. Rac2 and NFAT5 were up-regulated, while Cdc42 was down-regulated (**Figure 1**).

Western blotting of Cdc42, RAC1 and RAC2

To confirm the evidence of microarray and qPCR, we further detected CDC42, RAC1 and RAC2 protein levels by Western blotting. The alteration of CDC42 protein is consistent with the mRNA regulation in Aβ and Aβ with HupA treated cells. However, the changes of RAC2 are opposite to that of the mRNA level (**Figure 2**). Treatment with Aβ or HupA alone did not affect RAC1 obviously, but co-incubation of HupA (1, 10 μM) and Aβ markedly increased RAC1 level. The effect of HupA treated alone up-regulated the CDC42 and RAC2 protein which is inconsistent with changes of the mRNA levels.

Double immunofluorescence staining and neurite outgrowth analysis of Aβ-treated differentiated PC12 cells

To further confirm if the phenotype was affected by the alterations of the above-mentioned genes expression, we next studied the effect of Aβ on the NGF-induced neurite outgrowth. PC12 cell is a cell line from pheochromocytoma of the rat adrenal medulla. It differentiates in response to nerve growth factor (NGF) with a dramatic change in phenotype, acquiring biochemical and morphological characteristics of sympathetic neurons. The elaboration of neurites occurs within 24–48 h of NGF exposure and continues for up to a week [43]. Thus, PC12 cells have been widely used as a model system in the investigation of neuronal differentiation in vitro, esp. in neurite outgrowth [44, 45]. To determine the length of dendrite and axon, we performed double fluorescence staining (MAP-2 and Tau-1) followed by manually tracing the length analysis of NGF-induced PC12 cells. MAP-2 was used as a marker of dendrites, and Tau-1 as an axonal marker in neurons (**Figure 3A** and **4A**). Both MAP-2 and Tau-1 were mainly localized in the cell body (**Figure 3A** and **4A**). MAP-2 and Tau-1 positive neurites were almost undetectable in controls, but visualized in NGF-induced cells (**Figure 3A**). NGF (100 ng/ml) treatment induced neurite outgrowth in more than 60% of cells compared
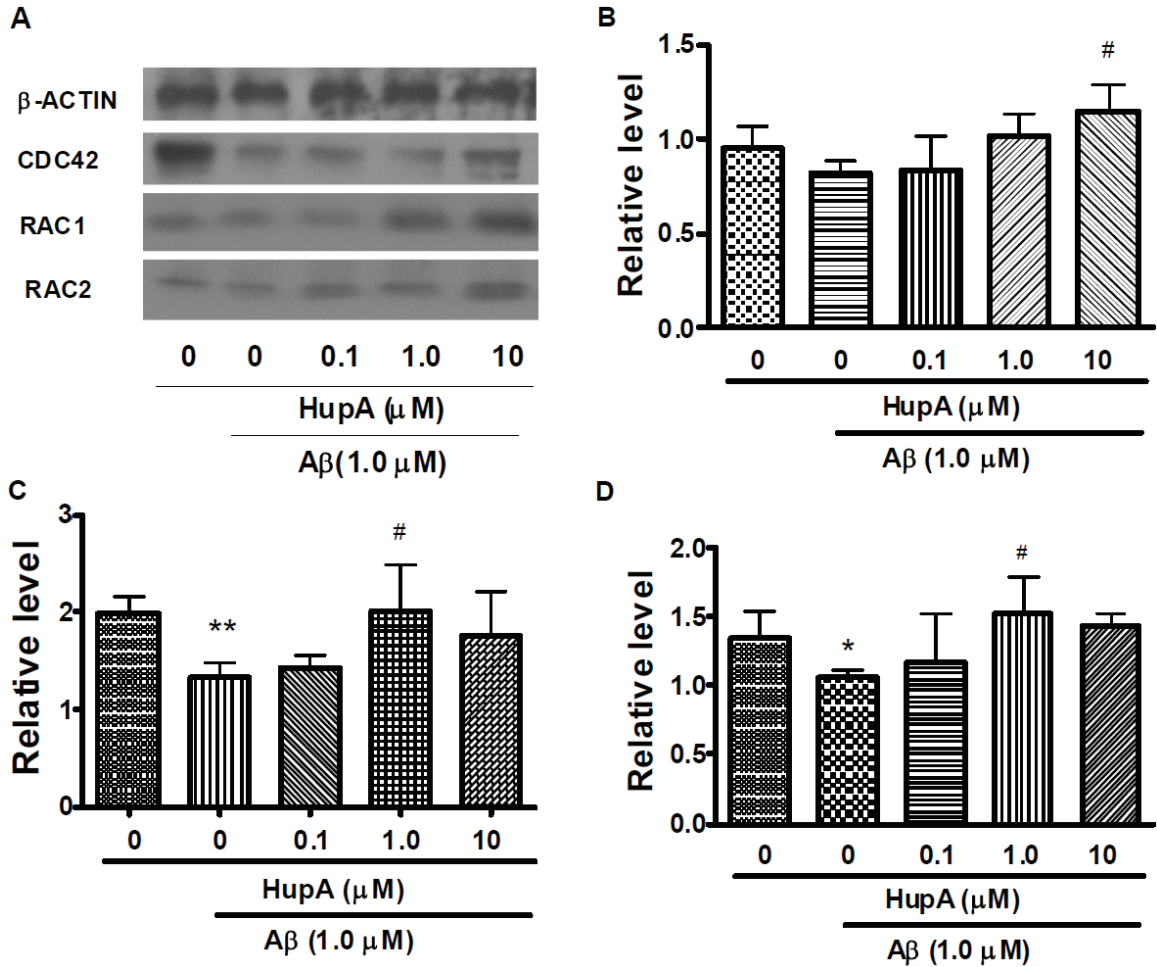
Figure 2. Western blotting analysis of CDC42, RAC1 and RAC2 protein levels in Aβ treated SH-SY5Y cells. After incubation with PBS, Aβ, HupA with Aβ for 24 h, SH-SY5Y cells were harvested and analyzed by western blot. Figure is the representative bands of β-ACTIN, CDC42, RAC1 and RAC2 Western blotting. A. Representative β-ACTIN, CDC42, RAC1 and RAC2 western blot bands. B, C and D. Immunoblots quantification of CDC42, RAC1 and RAC2, respectively. All bands were quantified and normalized by β-ACTIN. The data is expressed as mean ± SEM from three independent experiments. *p <0.05, **p <0.01 compared to control. #p < 0.05 compared to Aβ-treated group.

with control (**Figure 3**). Aβ treatment significantly reduced the number of neurite-bearing cells (**Figure 4B**) (reduced up to 35.63%, P<0.001) and shortened the neurite length (**Figure 4A**, **C**) compared to NGF control. These effects were markedly reversed by HupA (**Figure 4A**, **B** and **C**).

Discussion

The extension of axons and dendrites from the cell body is a complex and finely regulated process that requires the alteration of actin polymerization and depolymerization and tight dynamics of microtubules [46]. These events are under the control of various guidance cues and negative regulatory signals [47, 48]. PAK and ROCK are both the family of serine/threonine protein kinases. PAK involves in regulating the actin-severing protein cofilin, the actin cytoskeleton, and dendritic function as downstream effectors of Rac1/Cdc42 [49, 50]. By its kinase activity, ROCK regulates the activities of many target proteins (Rho, Rac, and Cdc42) which are involved in the regulation of cytoskeletal reorganization and then regulates dendrite initiation, growth, branching, spinogenesis, and spine maintenance [18, 51, 52].

The pheochromocytoma PC12 cell line has been used in both neurobiological [53] and neurotoxicological [53, 54] studies as a model
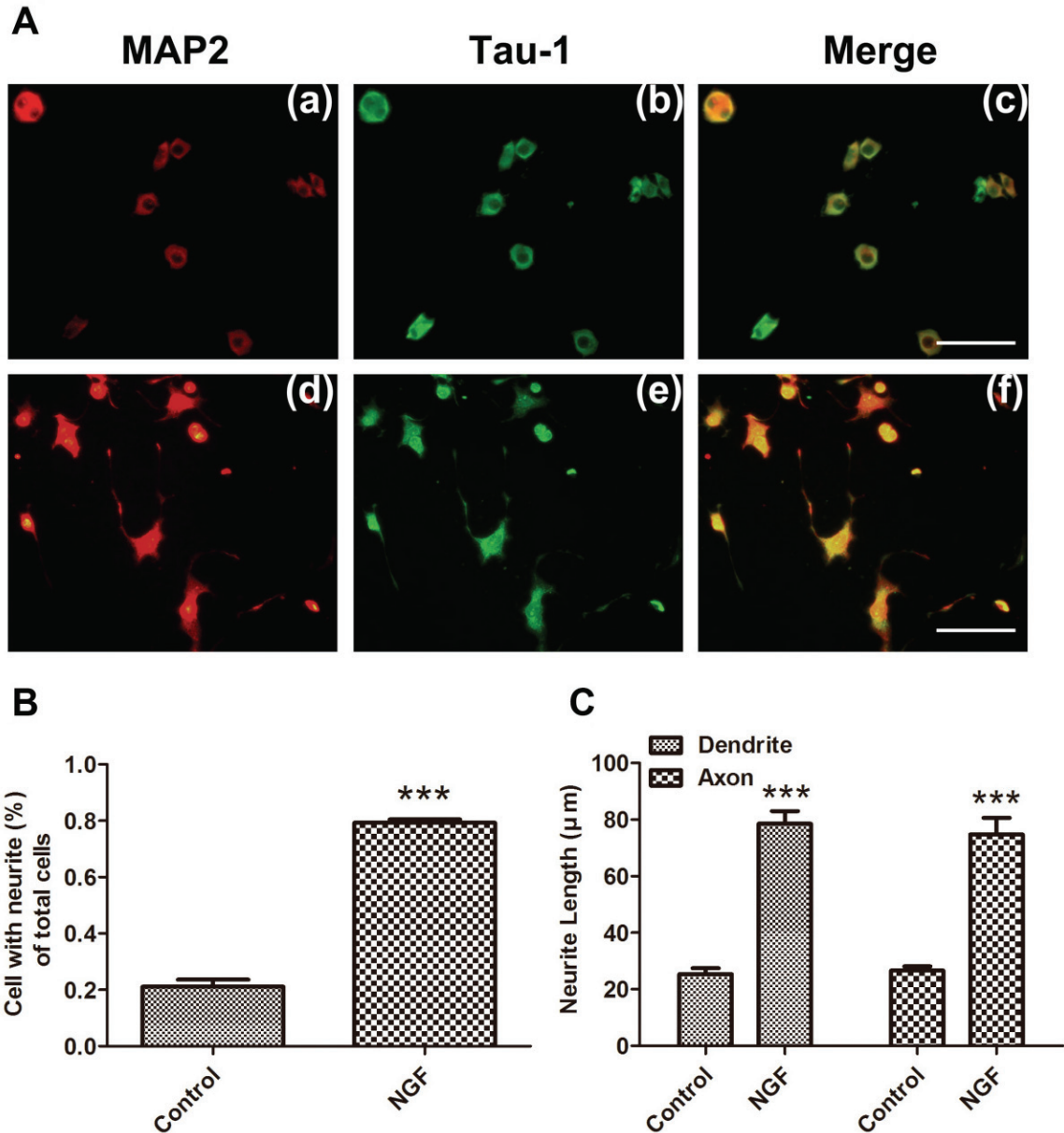
Figure 3. NGF induced PC12 cells differentiation. PC12 cells were induced with 100ng/ml NGF for 48h. A. Cells were untreated (a-c), treated with 100ng/ml NGF (d-f) for 48 hours prior to fixation and staining with anti-MAP-2 (red) (a, d) or anti-Tau-1 (green) (b, e). Merged images revealed both most colocalized in the cell bodies (c, f). B. Neurite formation was examined under a fluorescent microscope after immunofluorescent staining, and processes longer than one cell diameter were scored as neurites. C. The longest length of neurites per cell was measured after immunofluorescent staining, and the mean value of neurite length was calculated. ***p <0.001. Scale bar is 100 μm.

of neurite outgrowth. PC12 cells originate from chromaffin cells, whose differentiation into sympathetic neurons can also be induced by some factors including NGF, bFGF, and cAMP [55]. Previous reports studied that RhoA activity is correlated with neurite outgrowth in PC12 cells induced by cAMP [56], and Rab22 can promote nerve growth factor (NGF) signaling-dependent neurite outgrowth and gene expression in PC12 cells [57]. We described the method to quantify the number of neurites (dendrite and axon) bearing cells and neurite length after double immunofluorescence staining in PC12 cells using antibodies to Tau-1 as an axonal
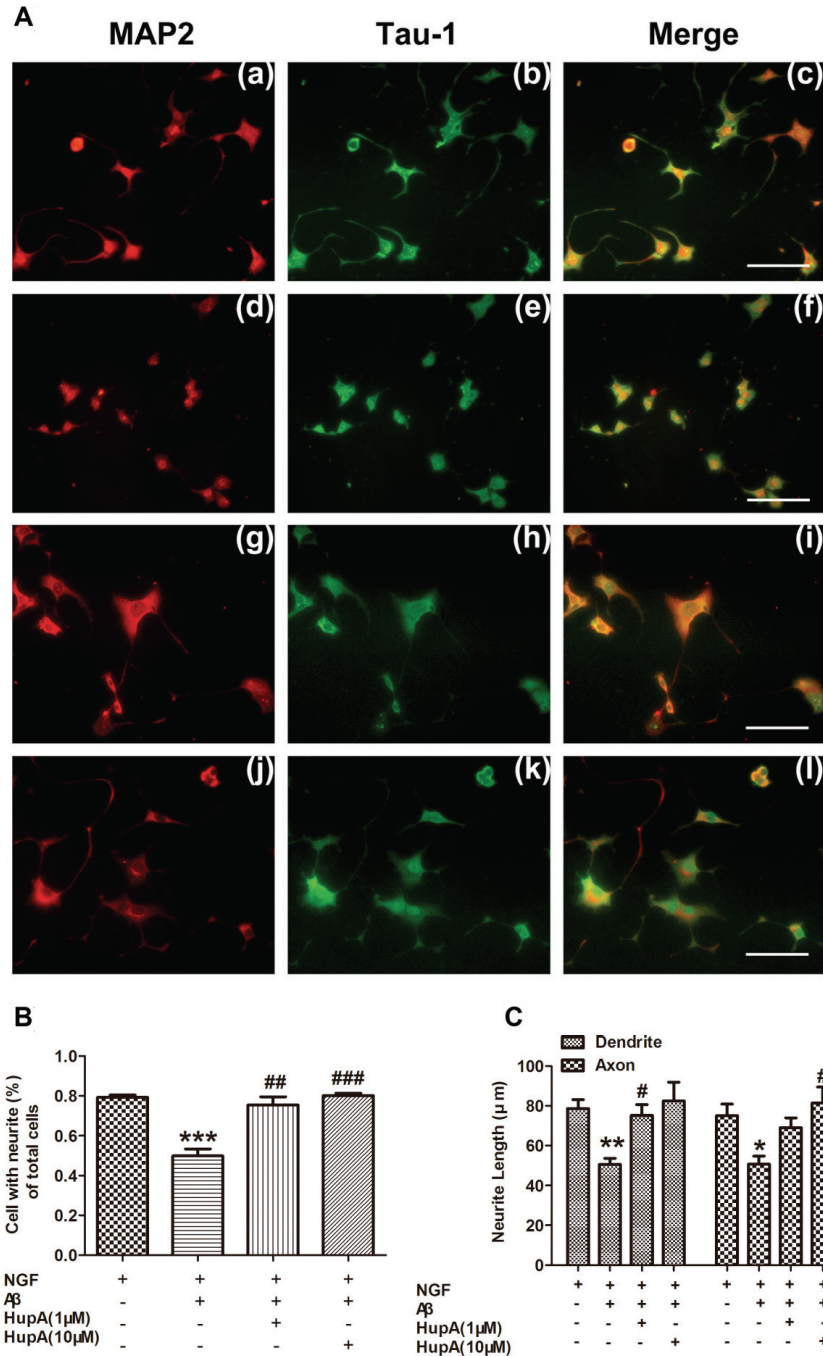
Figure 4. The effect of HupA on the NGF-induced neurite outgrowth of PC12 cells with Aβ treatment. Cells were treated with NGF (a-c), NGF and 1 μM Aβ1-42 (d-f), 1 μM (g-i) or 10 μM (j-l) HupA, respectively. HupA was added 2h before Aβ treatment A. shows the representative images of immunofluorescent staining under different treatments: MAP-2 (red) (a, d, g, j), Tau-1 (green) (b, e, h, k) and merged images revealed both (c, f, i, l). B. Neurite-bearing cells counting. Neurite formation is measured under a fluorescent microscope after immunofluorescent staining. The processes longer than one cell diameter were counted as neurites. C. The neurites length measurement. The longest length of neurites was measured after immunofluorescent staining, and the mean value of neurite length was calculated. Values are represented as means ±SEM. $^*p$ <0.05, $^{**}p$ <0.01 and $^{***}p$ <0.001 for comparisons between NGF treatment and co-treatment of NGF and Aβ; $^#p$ <0.05, $^{##}p$ <0.01 and $^{###}p$ <0.001 for comparisons between NGF and Aβ co-treated group and NGF, Aβ and Huperzine A co-treated group. Scale bar is 100 μm.

marker, and to MAP2 as a dendritic marker. Therefore the morphological changes are demonstrated in PC12 cells (**Figure 3** and **4**) to further confirm the result of microarray (**Table 2**), RT-PCR (**Figure 1**) and Western blotting (**Figure 2**). Our studies showed that Aβ regulates the genes expression involved in axon guidance in human neuroblastoma cells and inhibits NGF-induced neurite outgrowth in undifferentiated

PC12 rat pheochromocytoma cells (**Table 2**, **Figure 4**), which is agree with some of previous reports [58-61]. Aβ up-regulated the mRNA expressions of NFAT5, LIMK1, EPHA1, NTN4 and Rac2 markedly, but decreased Cdc42 expression. SEMA4F, PAK2 and Neural cell adhesion molecule L1 mRNA were not significantly regulated though a slight decrease was observed. All these factors are involved in the

pathways in regulation of actin cytoskeleton and axon guidance pathways. Our further immunofluorescence staining showing the inhibition of neurite outgrowth by Aβ (**Figure 4**) confirmed the consequences of the genes expression alteration. Previous reports indicated that PAK protein and activity are markedly reduced in Alzheimer's disease, and Aβ was directly involved in PAK signaling deficits [62]. Aβ-induced deficits showed an abnormal PAK activation and was accompanied by a rapid loss of F-actin and dendritic spines, which are the opposite responses compared to the normal activation of PAK by Rac/Cdc42 GTPase [4].

Even though a large number of reports have demonstrated the involvement of the Rho-ROCK pathway in the pathogenesis of several diseases [50], the pathogenesis of Rho GTPase pathways, esp. Rho-ROCK pathway, in AD development is still far less understood. In this study, Netrin4 (NTN4), the upstream factor of ROCK pathway was markedly up-regulated which suppose to activate ROCK signals. The result is agree with the previous report [63].

As a novel selective acetylcholinesterase inhibitor, HupA has been found, except for its potent AChE inhibition effect, to improve cognitive deficits in a broad range of animal models [33, 64-67] and to protect cells against cytotoxicity and apoptosis induced by multiple pathogenic factors [30, 32]. The mechanisms of these protective effects are still far less understood though we do find they related to attenuating oxidative stress [34, 35, 68, 69], regulating the apoptotic proteins [31, 33] and protecting mitochondria [70].

In this study, as shown in **Table 2**, **Figure 2** and **Figure 4**, co-incubation of Aβ and HupA reversed or decreased the changes of NFAT5, NTN4, RAC2, CDC42 and SEMA4F. HupA itself increased NFAT5, LIMK1, NTN4 significantly, but decreased RAC2, SEMA4F, PAK2 and LICAM. As a consequence, the Aβ-induced neurite outgrowth damage was declined with a dose response manner. The data implied that HupA might protect neurons morphologically and functionally, at least partially, against Aβ-induced pathological process via regulating neurite outgrowth and synaptogenesis. Our previous studies indicated that NGF and NGF receptors involved in HupA's non-cholinester-

ase inhibiting effects [30, 32]. It has been well known that NGF is the first neurotrophin to promote neuronal survival and differentiation [71]. Upon NGF induced neurite outgrowth, the NGF receptor TrkA activates several small G proteins, including Ras, Rap1, and the Cdc42-Rac1-RhoA family [72]. P75 low-affinity NGF receptor p75NTR modulates, in a ligand-dependent fashion, the activity of intracellular proteins known to regulate actin assembly [39]. Aβ activates the RhoA GTPase by binding to p75 NTR leading to impair the initial steps of NGF signaling, therefore inactivation of RhoA GTPase can protect cultured hippocampal neurons against the noxious effects of Aβ [73]. Our previous data shown that HupA markedly increased the number of neurite-bearing cells with a significant up-regulation of NGF and P75 low-affinity NGF receptor [38, 74]. From the study of hydrogen peroxide induced injury, the NGF and TrkA receptor mediate key events required for the neuroprotective actions of HupA. Among the downstream signaling events triggered by the action of NGF at the TrkA receptor, activation of the MAP/ERK kinase pathway may be particularly important for the ability of HupA to protect SH-SY5Y cells against oxidative stress [74]. The further data shown from present study agrees with the previous reports either from our study or the other's. It is very likely that the effect of HupA on the regulation of axon guidance relative genes and proteins related to affecting NGF signaling.

In addition to inhibiting AChE activity, in our previous study, AChE mRNA expression and protein levels were significantly upregulated after treatment with HupA [38]. Accumulating evidence indicates that AChE may influence neurite outgrowth through a non-catalytic mechanism. Via protein-protein interactions, AChE's effects on neurite outgrowth are not directly related to catalytic function but are nonetheless influenced by ligands with special structural features [75, 76]. Now that HupA increased AChE mRNA and protein levels, though the AChE activity was significantly inhibited [38], the effect of HupA on neurite outgrowth relative genes and proteins may be associated with the level of AChE expression.

Acknowledgement

Address correspondence to: Dr. Rui Wang, 130 Meilong Road, East China University of Science and Technology, Shanghai 200237, China. Tel/Fax: +86-21-64250823; E-mail: ruiwang@ecust.edu.cn

References

[1] Bartus RT, Dean RL, 3rd, Beer B and Lippa AS. The cholinergic hypothesis of geriatric memory dysfunction. Science 1982; 217: 408-414.

[2] Hyman BT and Tanzi RE. Amyloid, dementia and alzheimers-diseae. Current Opinion in Neurology and Neurosurgery 1992; 5: 88-93.

[3] Scheff SW, Dekosky ST and Price DA. Quantitative assessment of cortical synaptic density in alzheimers-disease. Neurobiology of Aging 1990; 11: 29-37.

[4] Ma QL, Yang FS, Calon F, Ubeda OJ, Hansen JE, Weisbart RH, Beech W, Frautschy SA and Cole GM. p21-activated kinase-aberrant activation and translocation in Alzheimer disease pathogenesis. Journal of Biological Chemistry 2008; 283: 14132-14143.

[5] Oostra BA and Willemsen R. FMR1: A gene with three faces. Biochimica Et Biophysica Acta-General Subjects 2009; 1790: 467-477.

[6] Steinbach P. Fragile X Syndrome. Medizinische Genetik 2009; 21: 251-259.

[7] Israely I, Costa RM, Silva AJ, Kosik KS and Liu X. Loss of delta - catenin changes synaptic composition and impairs plasticity and learning. Society for Neuroscience Abstract Viewer and Itinerary Planner 2003; 2003: Abstract No. 964.920.

[8] Small DH. Network dysfunction in Alzheimer's disease: does synaptic scaling drive disease progression? Trends in Molecular Medicine 2008; 14: 103-108.

[9] Bate C, Gentleman S and Williams A. alpha-synuclein induced synapse damage is enhanced by amyloid-beta1-42. Mol Neurodegener 2011; 5: 55.

[10] Bell KF and Claudio Cuello A. Altered synaptic function in Alzheimer's disease. Eur J Pharmacol 2006; 545: 11-21.

[11] Zheng ZQ, Sabirzhanov B and Keifer J. Oligomeric Amyloid-beta Inhibits the Proteolytic Conversion of Brain-derived Neurotrophic Factor (BDNF), AMPA Receptor Trafficking, and Classical Conditioning. Journal of Biological Chemistry 2010; 285: 34708-34717.

[12] Tampellini D, Capetillo-Zarate E, Dumont M, Huang ZY, Yu FM, Lin MT and Gouras GK. Effects of Synaptic Modulation on beta-Amyloid, Synaptophysin, and Memory Performance in Alzheimer's Disease Transgenic Mice. Journal of Neuroscience 2010; 30: 14299-14304.

[13] Lacor PN, Buniel MC, Chang L, Fernandez SJ, Gong YS, Viola KL, Lambert MP, Velasco PT, Bigio EH, Finch CE, Krafft GA and Klein WL. Synaptic targeting by Alzheimer's-related amyloid beta oligomers. Journal of Neuroscience 2004; 24: 10191-10200.

[14] Lacor PN, Buniel MC, Furlow PW, Clemente AS, Velasco PT, Wood M, Viola KL and Klein WL. A beta oligomer-induced aberrations in synapse composition, shape, and density provide a molecular basis for loss of connectivity in Alzheimer's disease. Journal of Neuroscience 2007; 27: 796-807.

[15] Li SM, Hong SY, Shepardson NE, Walsh DM, Shankar GM and Selkoe D. Soluble Oligomers of Amyloid beta Protein Facilitate Hippocampal Long-Term Depression by Disrupting Neuronal Glutamate Uptake. Neuron 2009; 62: 788-801.

[16] Shankar GM, Bloodgood BL, Townsend M, Walsh DM, Selkoe DJ and Sabatini BL. Natural oligomers of the Alzheimer amyloid-beta protein induce reversible synapse loss by modulating an NMDA-type glutamate receptor-dependent signaling pathway. Journal of Neuroscience 2007; 27: 2866-2875.

[17] Shankar GM, Li SM, Mehta TH, Garcia-Munoz A, Shepardson NE, Smith I, Brett FM, Farrell MA, Rowan MJ, Lemere CA, Regan CM, Walsh DM, Sabatini BL and Selkoe DJ. Amyloid-beta protein dimers isolated directly from Alzheimer's brains impair synaptic plasticity and memory. Nature Medicine 2008; 14: 837-842.

[18] Benarroch EE. Rho GTPases - Role in dendrite and axonal growth, mental retardation, and axonal regeneration. Neurology 2007; 68: 1315-1318.

[19] Huesa G, Baltrons MA, Gomez-Ramos P, Moran A, Garcia A, Hidalgo J, Frances S, Santpere G, Ferrer I and Galea E. Altered distribution of RhoA in Alzheimer's disease and AbetaPP overexpressing mice. J Alzheimers Dis 2010; 19: 37-56.

[20] Antoine-Bertrand J, Villemure JF and Lamarche-Vane N. Implication of rho GTPases in neurodegenerative diseases. Curr Drug Targets 2011; 12: 1202-1215.

[21] Chen LY, Rex CS, Babayan AH, Kramar EA, Lynch G, Gall CM and Lauterborn JC. Physiolog-

ical Activation of Synaptic Rac > PAK (p-21 Activated Kinase) Signaling Is Defective in a Mouse Model of Fragile X Syndrome. Journal of Neuroscience 2010; 30: 10977-10984.

[22] De Viti S, Martino A, Musilli M, Fiorentini C and Diana G. The Rho GTPase activating CNF1 improves associative working memory for object-in-place. Behavioural Brain Research 2010; 212: 78-83.

[23] Oh D, Han S, Seo J, Lee JR, Choi J, Groffen J, Kim K, Cho YS, Choi HS, Shin H, Woo J, Won H, Park SK, Kim SY, Jo J, Whitcomb DJ, Cho K, Kim H, Bae YC, Heisterkamp N, Choi SY and Kim E. Regulation of Synaptic Rac1 Activity, Long-Term Potentiation Maintenance, and Learning and Memory by BCR and ABR Rac GTPase-Activating Proteins. Journal of Neuroscience 2010; 30: 14134-14144.

[24] Svitkina T, Lin WH, Webb DJ, Yasuda R, Wayman GA, Van Aelst L and Soderling SH. Regulation of the Postsynaptic Cytoskeleton: Roles in Development, Plasticity, and Disorders. Journal of Neuroscience 2010; 30: 14937-14942.

[25] Narumiya S and Yasuda S. Rho GTPases in animal cell mitosis. Current Opinion in Cell Biology 2006; 18: 199-205.

[26] Hayashi K, Ohshima T and Mikoshiba K. Pak1 is involved in dendrite initiation as a downstream effector of Rac1 in cortical neurons. Molecular and Cellular Neuroscience 2002; 20: 579-594.

[27] Riento K and Ridley AJ. Rocks: Multifunctional kinases in cell behaviour. Nature Reviews Molecular Cell Biology 2003; 4: 446-456.

[28] Rajapaksha TW, Eimer WA, Bozza TC and Vassar R. The Alzheimer's beta-secretase enzyme BACE1 is required for accurate axon guidance of olfactory sensory neurons and normal glomerulus formation in the olfactory bulb. Mol Neurodegener 2011; 6: 88.

[29] Cao L, Rickenbacher GT, Rodriguez S, Moulia TW and Albers MW. The precision of axon targeting of mouse olfactory sensory neurons requires the BACE1 protease. Sci Rep 2012; 2: 231.

[30] Wang R, Yan H and Tang XC. Progress in studies of huperzine A, a natural cholinesterase inhibitor from Chinese herbal medicine. Acta Pharmacologica Sinica 2006; 27: 1-26.

[31] Wang R, Xiao XQ and Tang XC. Huperzine A attenuates hydrogen peroxide-induced apoptosis by regulating expression of apoptosis-related genes in rat PC12 cells. Neuroreport 2001; 12: 2629-2634.

[32] Wang R and Tang XC. Neuroprotective effects of huperzine A - A natural cholinesterase inhibitor for the treatment of Alzheimer's disease. Neurosignals 2005; 14: 71-82.

[33] Wang R, Zhang HY and Tang XC. Huperzine A attenuates cognitive dysfunction and neuronal degeneration caused by beta-amyloid protein-(1-40) in rat. European Journal of Pharmacology 2001; 421: 149-156.

[34] Xiao XQ, Wang R, Han YF and Tang XC. Protective effects of huperzine A on beta-amyloid (25-35) induced oxidative injury in rat pheochromocytoma cells. Neuroscience Letters 2000; 286: 155-158.

[35] Xiao XQ, Wang R and Tang XC. Huperzine A and tacrine attenuate beta-amyloid peptide-induced oxidative injury. Journal of Neuroscience Research 2000; 61: 564-569.

[36] Wang CY, Zheng W, Wang T, Xie JW, Wang SL, Zhao BL, Teng WP and Wang ZY. Huperzine A activates Wnt/beta-catenin signaling and enhances the nonamyloidogenic pathway in an Alzheimer transgenic mouse model. Neuropsychopharmacology 2011; 36: 1073-1089.

[37] Shigeta K, Ootaki K, Tatemoto H, Nakanishi T, Inada A and Muto N. Potentiation of nerve growth factor-induced neurite outgrowth in PC12 cells by a Coptidis Rhizoma extract and protoberberine alkaloids. Bioscience Biotechnology and Biochemistry 2002; 66: 2491-2494.

[38] Tang LL, Wang R and Tang XC. Effects of huperzine A on secretion of nerve growth factor in cultured rat cortical astrocytes and neurite outgrowth in rat PC12 cells. Acta Pharmacologica Sinica 2005; 26: 673-678.

[39] Yamashita T, Tucker KL and Barde YA. Neurotrophin binding to the p75 receptor modulates Rho activity and axonal outgrowth. Neuron 1999; 24: 585-593.

[40] Kaminsky YG, Marlatt MW, Smith MA and Kosenko EA. Subcellular and metabolic examination of amyloid-beta peptides in Alzheimer disease pathogenesis: evidence for Abeta (25-35). Exp Neurol 2010; 221: 26-37.

[41] Gulyaeva NV and Stepanichev MY. A beta (25-35) as proxyholder for amyloidogenic peptides: In vivo evidence. Experimental Neurology 2010; 222: 6-9.

[42] Farrer M, Kachergus J, Forno L, Lincoln S, Wang DS, Hulihan M, Maraganore D, Gwinn-Hardy K, Wszolek Z, Dickson D and Langston JW. Comparison of kindreds with parkinsonism and alpha-synuclein genomic multiplications. Annals of Neurology 2004; 55: 174-179.

[43] Das KP, Freudenrich TM and Mundy WR. Assessment of PC12 cell differentiation and neurite growth: a comparison of morphological and neurochemical measures. Neurotoxicol Teratol 2004; 26: 397-406.

[44] Khodagholi F, Tusi SK, Alamdary SZ, Amini M and Ansari N. 3-Thiomethyl-5,6-(dimethoxyphenyl)-1,2,4-triazine improves neurite out-

growth and modulates MAPK phosphorylation and HSPs expression in H(2)O(2)-exposed PC12 cells. Toxicology in vitro : an international journal published in association with BIBRA 2012; 26: 907-914.

[45] Labour MN, Banc A, Tourrette A, Cunin F, Verdier JM, Devoisselle JM, Marcilhac A and Belamie E. Thick collagen-based 3D matrices including growth factors to induce neurite outgrowth. Acta biomaterialia 2012; 8: 3302-3312.

[46] Boukhelifa M, Parast MM, Valtschanoff JG, LaMantia AS, Meeker RB and Otey CA. A role for the cytoskeleton-associated protein palladin in neurite outgrowth. Molecular Biology of the Cell 2001; 12: 2721-2729.

[47] Miller FD and Kaplan DR. Signaling mechanisms underlying dendrite formation. Current Opinion in Neurobiology 2003; 13: 391-398.

[48] Vaillant AR, Zanassi P, Walsh GS, Aumont A, Alonso A and Miller FD. Signaling mechanisms underlying reversible, activity-dependent dendrite formation. Neuron 2002; 34: 985-998.

[49] Ramakers GJA. Rho proteins, mental retardation and the cellular basis of cognition. Trends in Neurosciences 2002; 25: 191-199.

[50] Salminen A, Suuronen T and Kaarniranta K. ROCK, PAK, and Toll of synapses in Alzheimer's disease. Biochemical and Biophysical Research Communications 2008; 371: 587-590.

[51] Govek EE, Newey SE and Van Aelst L. The role of the Rho GTPases in neuronal development. Genes & Development 2005; 19: 1-49.

[52] Linseman DA and Loucks FA. Diverse roles of Rho family GTPases in neuronal development, survival, and death. Frontiers in Bioscience 2008; 13: 657-676.

[53] Radio NM, Breier JM, Shafer TJ and Mundy WR. Assessment of chemical effects on neurite outgrowth in PC12 cells using high content screening. Toxicol Sci 2008; 105: 106-118.

[54] Zhaleh H, Azadbakht M and Pour AB. Effects of extracellular calcium concentration on neurite outgrowth in PC12 cells by staurosporine. Neurosci Lett 2011; 498: 1-5.

[55] Sofroniew MV, Howe CL and Mobley WC. Nerve growth factor signaling, neuroprotection, and neural repair. Annu Rev Neurosci 2001; 24: 1217-1281.

[56] Jeon CY, Moon MY, Kim JH, Kim HJ, Kim JG, Li Y, Jin JK, Kim PH, Kim HC, Meier KE, Kim YS and Park JB. Control of neurite outgrowth by RhoA inactivation. J Neurochem 2012; 120: 684-698.

[57] Wang L, Liang Z and Li G. Rab22 controls NGF signaling and neurite outgrowth in PC12 cells. Mol Biol Cell 2011; 22: 3853-3860.

[58] Magara F, Muller U, Li ZW, Lipp HP, Weissmann C, Stagljar M and Wolfer DP. Genetic background changes the pattern of forebrain commissure defects in transgenic mice underexpressing the beta-amyloid-precursor protein. Proceedings of the National Academy of Sciences of the United States of America 1999; 96: 4656-4661.

[59] Zou YM. Axons find their way in the snow. Development 2009; 136: 2135-2139.

[60] Caltagarone J, Hamilton RL, Murdoch G, Jing Z, DeFranco DB and Bowser R. Paxillin and Hydrogen Peroxide-Inducible Clone 5 Expression and Distribution in Control and Alzheimer Disease Hippocampi. Journal of Neuropathology and Experimental Neurology 2010; 69: 356-371.

[61] Wilkinson B, Koenigsknecht-Talboo J, Grommes C, Lee CYD and Landreth G. Fibrillar beta-amyloid-stimulated intracellular signaling cascades require Vav for induction of respiratory burst and phagocytosis in monocytes and microglia. Journal of Biological Chemistry 2006; 281: 20842-20850.

[62] Zhao LX, Ma QL, Calon F, Harris-White ME, Yang FS, Lim GP, Morihara T, Ubeda OJ, Ambegaokar S, Hansen JE, Weisbart RH, Teter B, Frautschy SA and Cole GM. Role of p21-activated kinase pathway defects in the cognitive deficits of Alzheimer disease. Nature Neuroscience 2006; 9: 234-242.

[63] Petratos S, Li QX, George AJ, Hou X, Kerr ML, Unabia SE, Hatzinisiriou I, Maksel D, Aguilar MI and Small DH. The beta-amyloid protein of Alzheimers disease increases neuronal CRMP-2 phosphorylation by a Rho-GTP mechanism. Brain 2008; 131: 90-108.

[64] Ou LY, Tang XC and Cai JX. Effect of huperzine A on working memory in reserpine- or yohimbine-treated monkeys. European Journal of Pharmacology 2001; 433: 151-156.

[65] Wang LM, Han YF and Tang XC. Huperzine A improves cognitive deficits caused by chronic cerebral hypoperfusion in rats. European Journal of Pharmacology 2000; 398: 65-72.

[66] Wang LS, Zhou J, Shao XM and Tang XC. Huperzine A attenuates cognitive deficits and brain injury in neonatal rats after hypoxia-ischemia. Brain Research 2002; 949: 162-170.

[67] Xiong ZQ, Cheng DH and Tang XC. Effects of huperzine A on nucleus basalis magnocellularis lesion-induced spatial working memory deficit. Acta Pharmacologica Sinica 1998; 19: 128-132.

[68] Xiao XQ, Yang JW and Tang XC. Huperzine A protects rat pheochromocytoma cells against hydrogen peroxide-induced injury. Neuroscience Letters 1999; 275: 73-76.

[69] Xiao XQ, Zhang HY and Tang XC. Huperzine A attenuates amyloid beta-peptide fragment 25-35-induced apoptosis in rat cortical neu-

rons via inhibiting reactive oxygen species formation and caspase-3 activation. Journal of Neuroscience Research 2002; 67: 30-36.

[70] Zhou J and Tang XC. Huperzine A attenuates apoptosis and mitochondria-dependent caspase-3 in rat cortical neurons. Febs Letters 2002; 526: 21-25.

[71] Levimontalcini R. The nerve growth-factor 35 years later. Science 1987; 237: 1154-1162.

[72] Huang EJ, Zang KL, Schmidt A, Saulys A, Xiang MQ and Reichardt LF. POU domain factor Brn-3a controls the differentiation and survival of trigeminal neurons by regulating Trk receptor expression. Development 1999; 126: 2869-2882.

[73] Chacon PJ, Garcia-Mejias R and Rodriguez-Tebar A. Inhibition of RhoA GTPase and the subsequent activation of PTP1B protects cultured hippocampal neurons against amyloid beta toxicity. Mol Neurodegener 2011; 6: 14.

[74] Tang LL, Wang R and Tang XC. Huperzine A protects SHSY5Y neuroblastoma cells against oxidative stress damage via nerve growth factor production. European Journal of Pharmacology 2005; 519: 9-15.

[75] Brimijoin S and Koenigsberger C. Cholinesterases in neural development: New findings and toxicologic implications. Environmental Health Perspectives 1999; 107: 59-64.

[76] Brimijoin S. Can cholinesterase inhibitors affect neural development? Environmental Toxicology and Pharmacology 2005; 19: 429-432.